FROM THE DEPARTMENT OF RADIATION PHYSICS (DIRECTOR: PROF. K. LIDÉN),
UNIVERSITY OF LUND, SWEDEN.

DOSIMETRIC STUDIES OF MANTLE FIELDS IN COBALT 60 THERAPY OF MALIGNANT LYMPHOMAS

by

GUDRUN SVAHN-TAPPER

During the past few years an increasing number of radiotherapists have advocated a particular type of radiation treatment for certain forms of lymph node diseases, a significantly larger portion of the body being subjected to radiation than was previously customary. These conditions which were formerly regarded as generalized are now considered to be initially local and therefore possibly curable (CRAVER 1954, KAPLAN 1962, 1966, EASSON & RUSSEL 1963, PETERS 1966 and MUSSHOFF & BOUTIS 1968). It has also been demonstrated that the spread is often at first to the adjacent lymph node groups (JELLIFFE 1965, NEWALL 1965, KAPLAN 1966, ROSENBERG & KAPLAN 1966, LANDBERG & LARSSON 1968, LANDBERG 1969). The best results of treatment should therefore be attained if the clinically involved lymph node groups as well as adjacent groups are irradiated. The submandibular, cervical, supraclavicular, infraclavicular, axillary and mediastinal lymph node groups are consequently all irradiated in supradiaphragmatic conditions. The simplest technique for such treatment is the use of two large opposing anterior and posterior fields with lead blocks interposed to shield tissues not to be irradiated. Large source to skin distances are necessary and the treatment fields are irregular in shape.

Submitted for publication 26 June 1969.

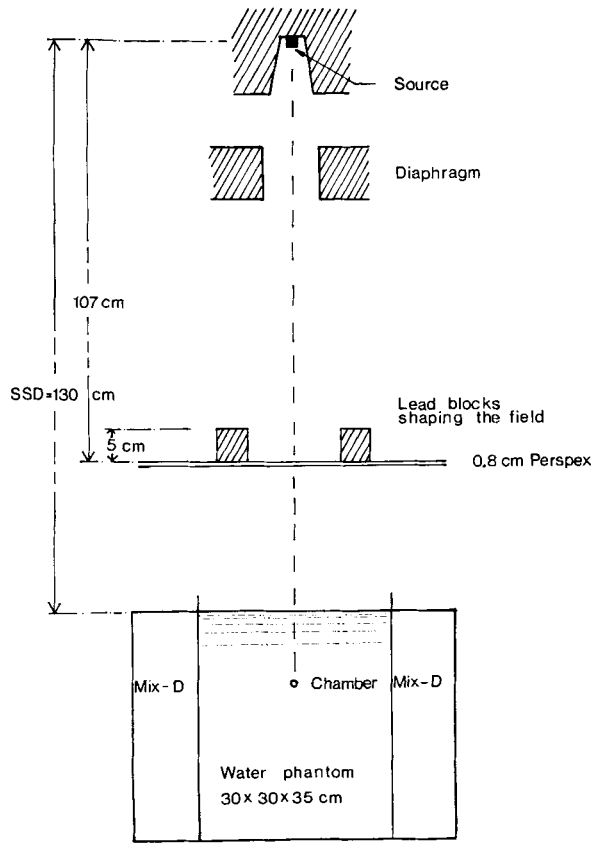

Fig. 1. Schematic drawing of apparatus for the determination of depth doses in different parts of the mantle field. The clinical situation is simulated by exchanging the water phantom and mix-D blocks for the thorax phantom.

This report describes isodose charts for a sagittal plane in the centre of the field with and without a beam flattening filter, and for transverse planes at the levels of the jugulum and the pulmonary hila. A comparison between planned dose distribution and measured dose at certain points in a thorax phantom is also presented.

Material and Methods

Experimental equipment. The measurements were carried out with a Siemens Gammatron III, which has a cobalt 60 source with a diameter of 1.5 cm. The cobalt 60 unit is equipped with a block diaphragm, its anterior part being 23.8 cm from the source. The edge of the light beam was adjusted to match the 50 % isodose line at 0.5 cm depth, for a field size of 10 cm $\times$ 10 cm. All

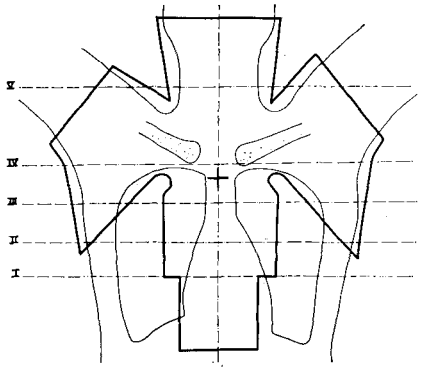

Fig. 2. Mantle field with reference to thorax phantom. Dotted lines indicate planes where dose planning and measurements are carried out.

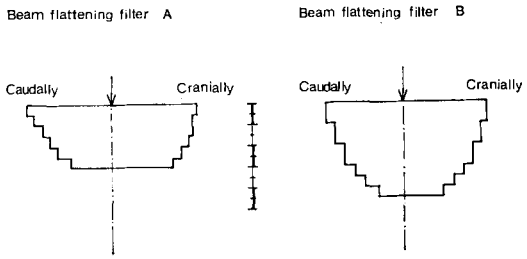

Fig. 3. The two beam-flattening filters A and B are made of perspex with a density of 1.18 kg/cm^3; source-filter distance: 30.2 cm.

measurements were carried out at an SSD of 130 cm. The beam direction was vertical.

Phantoms used in the measurements. All depth dose measurements were performed in a 30 cm × 30 cm × 35 cm water phantom, and with mix-D as side-scattering material where the phantom was not sufficiently large. The film exposure for dose determination was made in a polystyrene phantom 35 cm × 35 cm × 30 cm, also with mix-D as side-scattering material. The thorax phantom consisted of mix-D and contained a skeleton, the arms being above the head with the neck extended. The lungs were filled with sawdust to a density of 0.25 g/cm^3, which according to DAHL & VIKTERLÖF (1960) is the radiation equivalent of an air-filled lung. Unfortunately, the chest wall of the phantom was too thick and the apices of the lungs terminated at the jugulum instead of at Th2.

Beam-flattening filters. The beam-flattening filters used in the cranial-caudal direction were made up of perspex plates, 0.5 cm thick, with a density of 1.18 g/cm^3. The source-filter distance was 30.2 cm (see Fig. 3).

Shape and size of the mantle field. The mantle field was formed of 5 cm lead blocks placed on a 0.8 cm perspex plate 107 cm from the cobalt source (Fig. 1). The sides of the lead blocks were vertical and the shape and size of the mantle field were adjusted to simulate a mantle treatment; the size of the field before the lead blocks were interposed was 38 cm × 40 cm. The mantle

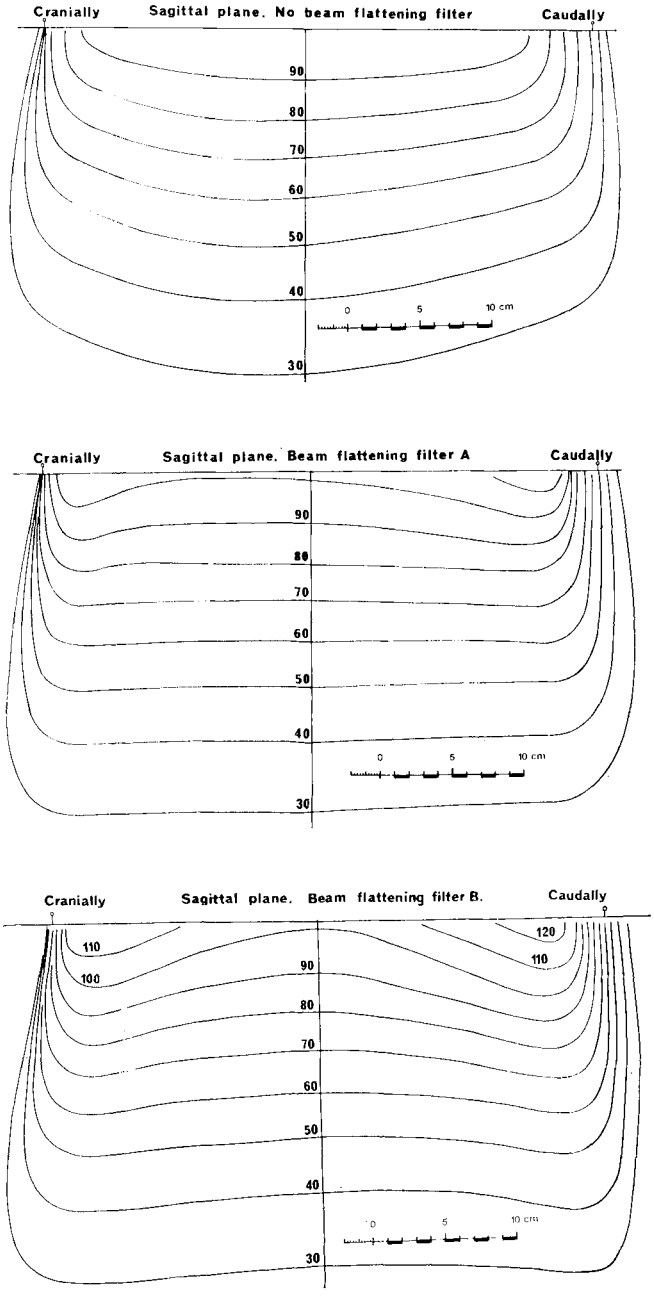

Fig. 4. Isodose charts for the sagittal plane in the middle of the mantle field: without beam-flattening filter (upper), and, respectively, with beam-flattening filter A (middle) and filter B (lowermost).

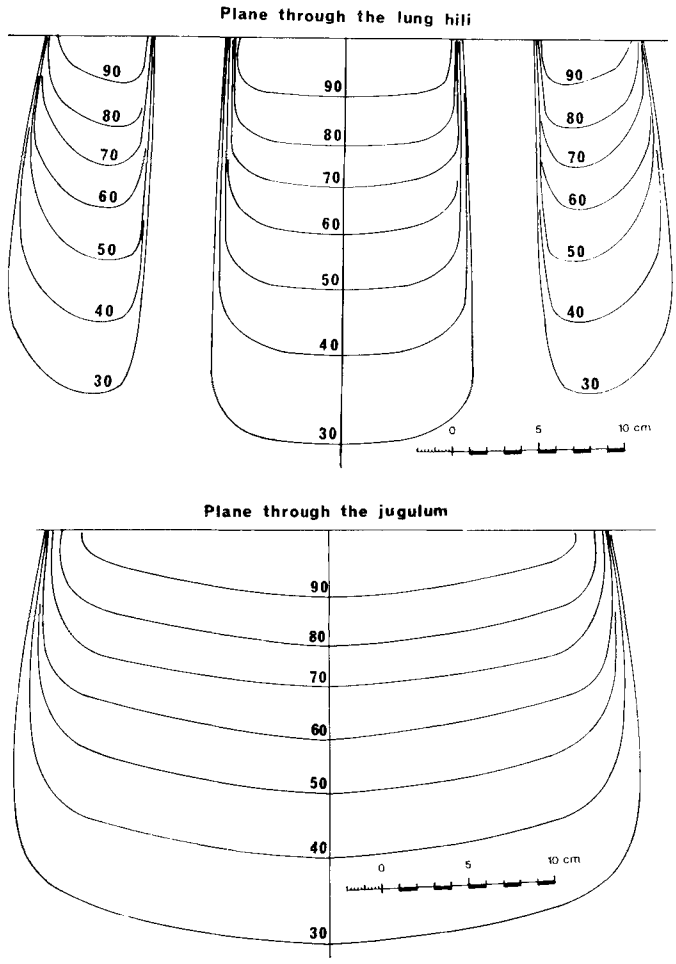

Fig. 5. Isodose charts for transverse planes according to fig. 2; no beam-flattening filter in either direction.

field was so formed (Fig. 2) that the light beam indicated a border of 1 cm outside the target area, projected vertically onto the surface of the phantom where the target area included all supradiaphragmal lymph nodes from the mastoid process to Th12. The primary field extension outside the target was 3 cm, 2 cm of which were shielded by lead on the cranial and lateral borders. The broad penumbra was left undiminished on the caudal border to facilitate the addition of abdominal fields. With depth dose measurements for square fields, the size of the field was defined by the diaphragm of the cobalt unit.

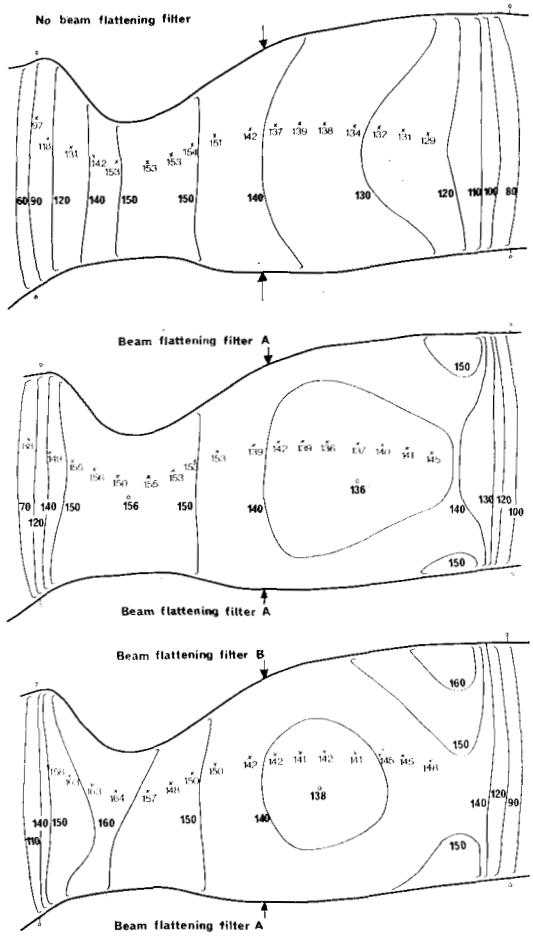

Fig. 6. Dose planning for anterior and posterior fields in the sagittal plane through the middle of the phantom respectively without and with beam-flattening filters. X indicates dose values measured with condenser chambers. The trachea is filled with paraffin pellets.

Measuring procedure. Depth dose measurements for all the fields were made with the aid of a cable-connected ionization chamber, the air volume of which was 1.0 cm^3. An ionization chamber of air-volume 0.1 cm^3, cable connected, was also used in the determination of depth doses for field sizes 10 cm $\times$ 10 cm and 17 cm $\times$ 17 cm. All the ionization chambers were calibrated free in air against a substandard chamber which had in turn been calibrated at the Standard Laboratory of the Swedish Radiation Protection Institute. When the ionization

chambers are used for dose measurements at different depths in a phantom, the photon spectrum differs considerably from the spectrum free in air, and the secondary radiation is almost isotropically incident on the ionization chamber. Photon-spectra for different depths and for different field sizes are reproduced in the diagram of BRUCE & JOHNS (1960).

According to calculations, the equivalent area to the mantle field is approximately 25 cm × 25 cm. The calibration constant for the ionization chamber of volume 1.0 cm^3 determined free in air varied less than 2 % for HVL 0.2 mm Cu to HVL 14.6 mm Cu. Thus, no corrections for energy dependence were made and the possible direction dependence for cobalt radiation could be ignored. In measurements with the ionization chamber of volume 0.1 cm^3 these two factors were eliminated through a comparative measurement using the same field size at a SSD of 100 cm for which depth doses are known (Brit. J. Radiol. 1961). The difference in the depth dose measurements of the small and large ionization chambers was 2 % of the measured value for a depth of 20 cm, after standardizing to 5 cm depth. Depth dose measurements in water for mantle fields were also carried out by means of a Fricke dosimeter. The volume of the dosimeter was 4 ml.

Depth dose measurements made in eight different radiation directions, distributed evenly over the mantle field, form the basis for the determination of isodose charts. Measurements were carried out with the aid of the cable-connected ionization chamber of volume 1.0 cm^3. Supplementary measurements were made with condenser chambers of volume 0.3 cm^3 at depths of 5 cm and 15 cm. Film dosimetry was used for further help in drawing the isodose lines. It proved to be impossible to obtain a linear relationship between film density and exposure within the whole mantle field, since the energy spectrum differs between the central and distal parts of the field. Isodensity lines were therefore used only for the distal parts of the field, where an explicit relationship between density and exposure could be obtained. In the other parts of the mantle field they were used only as an aid in drawing the isodose lines between the dose values measured by the ionization chamber.

The thorax phantom was dose-planned centrally in a sagittal plane both with and without beam-flattening filter, as shown in Fig. 6, and in five transverse planes as seen in Figs 7—11. Correction for irregular body contour was made with the isodose shift method (DUTREIX & DUTREIX 1962). In the axillary and submandibular regions, the isodoses were shifted in the direction of the divergence of the local beam. The dose measurements in these transverse planes as well as in the oesophagus were carried out with the aid of condenser chambers.

All figures in the isodose charts and dose planes are written on the higher dose side of the isodose line.

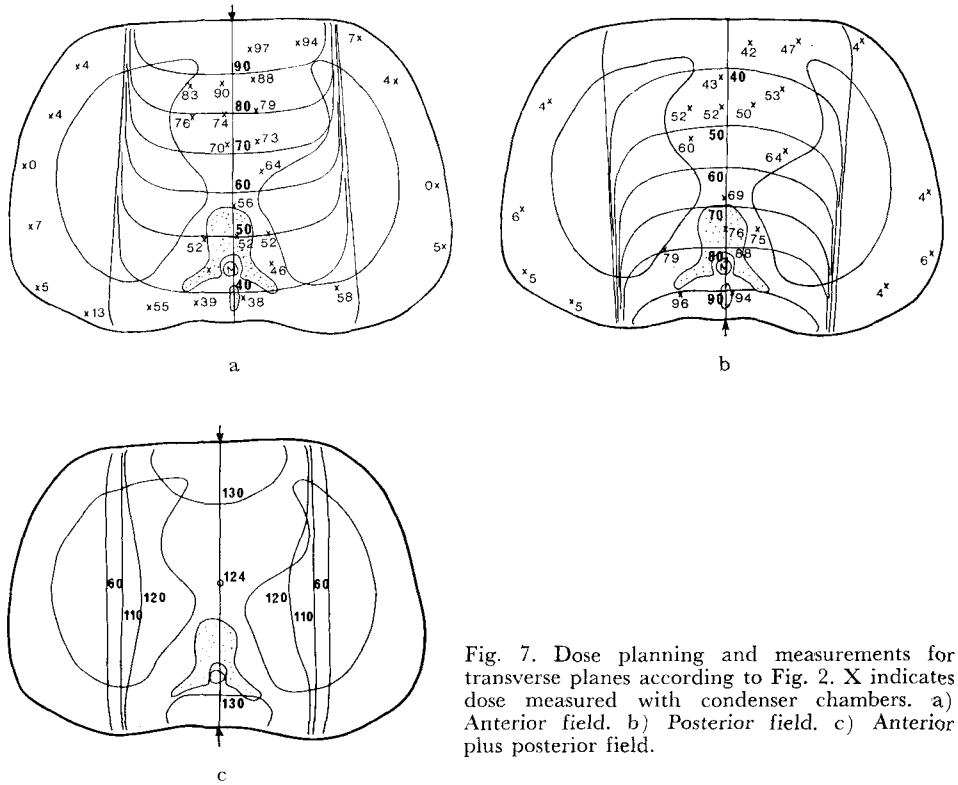

Fig. 7. Dose planning and measurements for transverse planes according to Fig. 2. X indicates dose measured with condenser chambers. a) Anterior field. b) Posterior field. c) Anterior plus posterior field.

Results and Discussion

Calculation of depth dose. The depth dose for SSD = 130 cm has been calculated for field sizes 0 cm^2, 10 cm × 10 cm, 17 cm × 17 cm and 20 cm × 20 cm, according to the British Journal of Radiology (1961), Suppl. No 10. The tissue/air ratio measured by GUPTA & CUNNINGHAM (1966) was used in the calculation. Depth dose calculations for the mantle field were made according to the method of CLARKSON (1941). The field was then divided into sectors of 5°. The scatter function, according to GUPTA & CUNNINGHAM (1966), is given as

$$S(r_x,d,F) = 100\left(\frac{F+x}{F+d}\right)^2 \left[T(r_d,d) - \exp\{-\mu(d-x)\}\right]$$

where the scatter function is defined as the dose due to scattered radiation at points along the central axis of the beam per 100 rad, from primary radiation

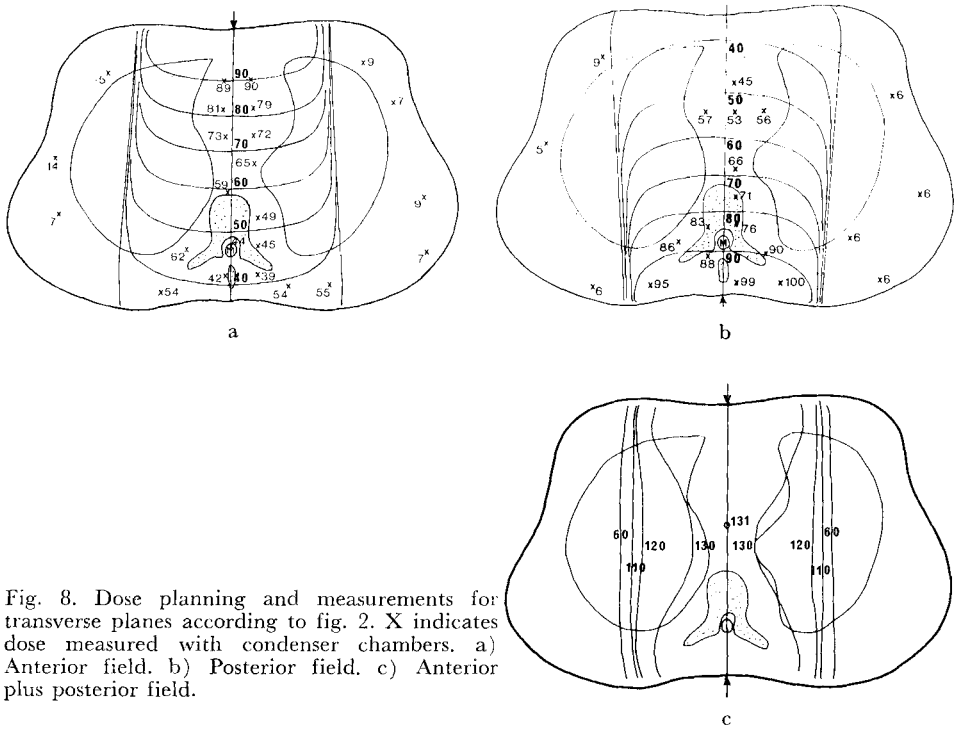

Fig. 8. Dose planning and measurements for transverse planes according to fig. 2. X indicates dose measured with condenser chambers. a) Anterior field. b) Posterior field. c) Anterior plus posterior field.

alone, at the position of the maximum dose in the phantom; x is the depth of maximum dose; r_x the radius a circular beam would have at depth x; F is the SSD; $T(r_d,d)$ is the tissue/air ratio for depth d in the phantom and μ is the narrow-beam attenuation coefficient for the phantom material.

Since the tissue/air ratio is independent of SSD, $S(r_x,d,130)$ may be written

$$S(r_x,d,130) = \frac{\left(\frac{130\cdot 5}{130+d}\right)^2}{\left(\frac{80\cdot 5}{80+d}\right)^2} \cdot S(r_x',d,80)$$

$$\text{where } r_x' = \frac{80\cdot 5}{80+d} \cdot \frac{130+d}{130\cdot 5} \cdot r_x$$

Scatter functions for SSD = 80 cm have been tabulated by the same authors. Calculation of the depth dose is made for the centre of the field (Table 1) and for a point 11.6 cm below the centre. The scatter function for the mantle field has the same value as for a square of 25 cm × 25 cm.

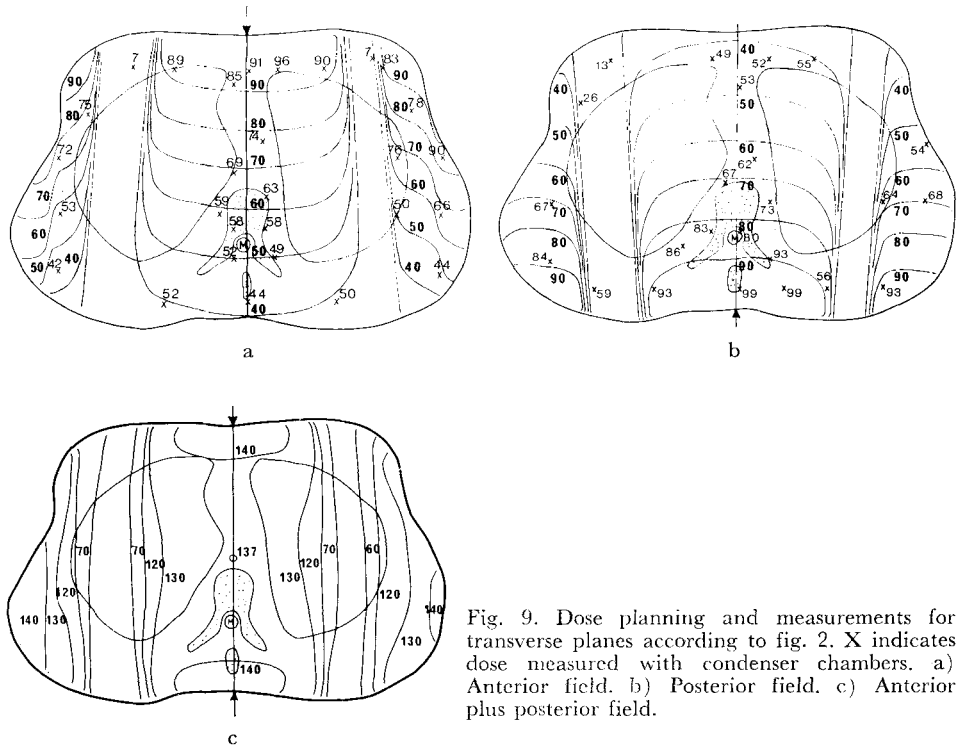

Fig. 9. Dose planning and measurements for transverse planes according to fig. 2. X indicates dose measured with condenser chambers. a) Anterior field. b) Posterior field. c) Anterior plus posterior field.

For the point below the centre the calculated dose at a depth of 10 cm is 62.5 % and the dose measured with the ionization chamber 61.8 %. If the field is 4 cm longer in a caudal direction, the calculated dose at 10 cm is 63.1 %, and if the field is shortened 4 cm caudally the calculated dose becomes 61.3 %.

Comparison between calculated and measured depth dose. A comparison is made in Table 1 between measured and calculated values of depth doses, the former being standardized to those calculated at 5 cm. The mean values of measurements with two ionization chambers are entered in the table for the fields 10 cm × 10 cm and 17 cm × 17 cm. The uncertainty in the Fricke measurements at a depth of 14.6 cm is ± 5 % of the depth dose value. The difference in measured and calculated values for greater depths may possibly depend on the difference in the back-scattering material. At 20 cm depth, 10.7 cm of phantom material lay behind the ionization chamber, while the tissue/air ratios and scatter functions were determined in a water phantom that was 60

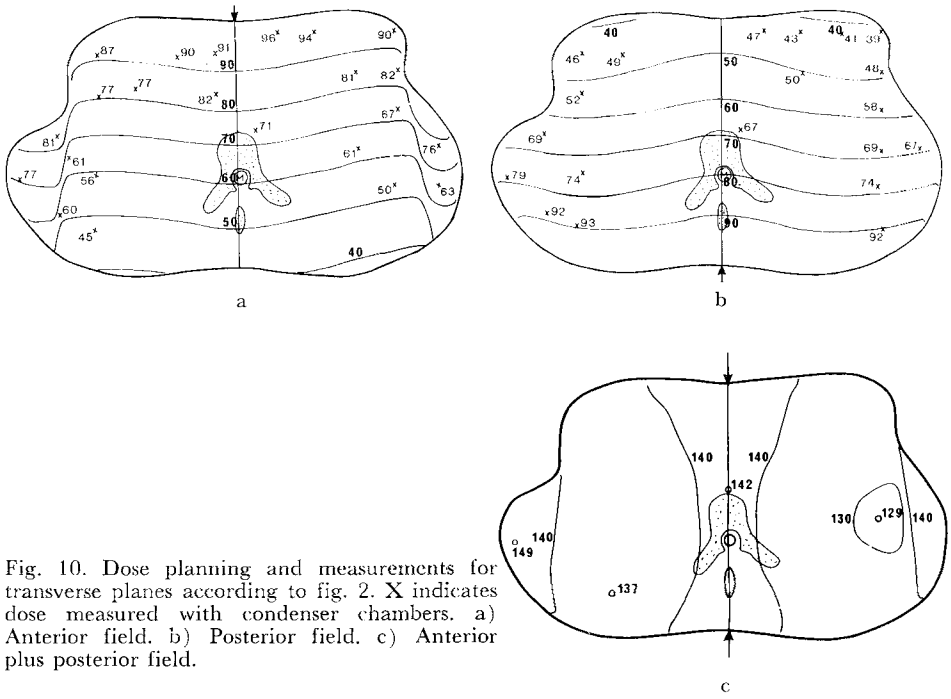

Fig. 10. Dose planning and measurements for transverse planes according to fig. 2. X indicates dose measured with condenser chambers. a) Anterior field. b) Posterior field. c) Anterior plus posterior field.

cm deep. The measured values have been used in the isodose charts but standardized to 100 % at 0.5 cm depth.

Dose rate variation according to the shape and size of the mantle fields. The mantle field must be modified individually in the treatment of patients and therefore the shape and size may differ from one patient to another. The measurements were made in a water phantom representing two extreme fields, the one in a child of 12 years (157 cm, 41 kg) and the other in a male adult (190 cm, 100 kg). The measurements were carried out in the centre, and the back scatter material was the same for all fields. A comparative measurement in which the hilar region was covered with lead blocks was also performed. The results are presented in Table 2.

Isodose charts. Isodose charts centrally in a sagittal plane are shown in Fig. 4, and for transverse planes at respectively the hilar and jugulum levels in Fig. 5. The depth dose in the transverse planes was adjusted to the depth dose in the sagittal plane at the corresponding level. Two beam-flattening filters (cf. Fig. 3) were made for the sagittal plane. Since the patient always

Table 1

Calculated and measured percentage depth doses for SSD = 130 cm — The measured depth doses are standardized to the calculated doses at 5 cm

Depth in cm	Field sizes						Mantle field equivalent to square 25 cm × 25 cm		
	10 cm × 10 cm		17 cm × 17 cm		20 cm × 20 cm				
	Calculated	Measured, ionization chamber	Calculated	Measured, ionization chamber	Calculated	Measured, ionization chamber	Calculated	Measured, ionization chamber	Measured, Fricke dosimeter
0.5	100	98.6	100	98.9	100	98.5	100	99.2	
1.0								99.2	
2.0	94.9		95.5		95.7				
5.0	81.9	81.9	83.9	83.9	84.4	84.4	84.8	84.8	84.8
9.8							67.4		67.4
10.0	60.3	60.5	64.1	64.4	65.2	65.3	66.6	67.0	
14.6							51.7		52.5
15.0	43.4	44.4	47.9	49.1	49.2	49.4	51.1	50.6	
20.0	31.2	30.7	35.8	36.4	37.2	36.8	39.1	37.7	

Table 2

Comparison of the dose rates in the central line of mantle fields of different sizes

Depth cm	Field suiting the phantom including hila	Field suiting the phantom excluding hila	Field suiting a small patient including hila	Field suiting a tall patient including hila
5	100	98.5	98.9	101.2
15	51.0	49.6	50.0	52.0

has a greater antero-posterior thickness in the submandibular and mediastinal regions, as compared to the jugulum level, the filters are overcompensating to produce as homogeneous a dose as possible to the whole target volume. The depth dose at less than 20 cm depth in the centre of the field with beam-flattening filters does not differ from the depth dose without filter.

Comparison of planned and measured dose in a thorax phantom. The upper charts (a and b) in Figs 7, 8, 9 and 10 indicate the planned and the measured dose values, respectively, for both the anterior and the posterior treatment fields in the transverse planes I to IV as in Fig. 2. Measurements and dose

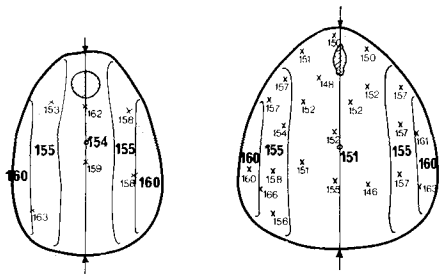

Fig. 11. Dose planning and measurements for two phantoms of the neck differing in size. X indicates the dose measured with condenser chambers. Air in trachea.

planning were carried out for two different phantoms of the neck, since the neck contour of patients often differs considerably (Fig. 11). The trachea was filled with paraffin pellets in the oesophagus measurements (Fig. 6). Measurements made with air in the trachea, where the diameter of the air cavity was 16 mm, produced a 7 % increase in the hypopharynx and the oesophagus versus the subcutaneous maximum dose in the centre of the ventral field. Thus, to obtain the best possible interpretation of the measured values in the hypopharynx and the oesophagus, the position of the catheter with ionizing chambers, in relation to the trachea, should always be determined with the aid of a film exposed during the treatment.

A statistical analysis of the accuracy of the measured values is difficult to carry out, since systematic errors are introduced. For example, no correction was made for inhomogeneous tissue and the correction for the body contour was made with the isodose shift method, even when the angle of incidence was more than 45°. No consideration was made for the smaller mass of the side-scattering material in the thorax phantom measurements as compared with the water phantom measurements. The accuracy of the ionization chamber

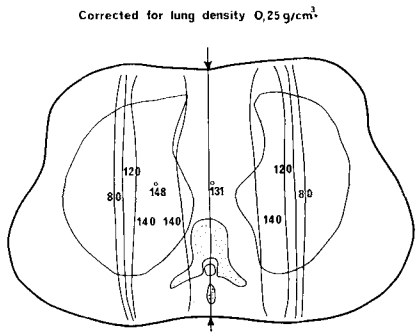

Fig. 12. Dose planning in the hilar region for anterior and posterior fields with correction for lung density 0.25 g/cm³. (Cf. fig. 8 c.)

measurements is ± 4 % of the measured value; this figure includes an energy dependence of about 1 %.

Lung correction at the hilar level. To calculate the lung correction, the ionization chamber measurements were performed for the anterior field at four different lung depths at the hilar level. If the depth dose curve in water for the mentioned level in the mantle fields is drawn as a straight line in a semi-logarithmic diagram, for depths greater than 5 cm, the measurements in the lung, plotted in the same diagram, follow a line with a slope of 0.6 compared with the depth dose decrease in water.

The isodose distribution at the hilar level with lung correction is indicated in Fig. 12 (cf. Fig. 8c).

Conclusion

In spite of all uncertainties introduced in the treatment planning of the thorax phantom, the agreement with the dose measured at certain points is surprisingly good. In the mantle treatment of patients it should therefore be sufficient to control the dose in the sagittal plane by measurements in the hypopharynx and oesophagus for checking the effect of the field size, the patient's size and the possible movements of viscera between the two treatment positions.

To obtain as homogeneous a dose as possible in the whole target area, a beam flattening filter should be used in a cranial-caudal direction, with an individual filter in the cervical region. The hilar regions of the lungs should be shielded with lead during some of the treatments to prevent a too high dose to the lungs.

SUMMARY

The dosimetry for mantle fields in the treatment of supradiaphragmatic malignant lymphomas with cobalt 60 was analysed. Isodose charts for the mantle field were constructed in sagittal and in different transverse planes. Studies of the agreement between planned and measured doses in a thorax phantom were performed both with and without beam flattening filters.

ZUSAMMENFASSUNG

Die dosimetrischen Grundlagen für Mantelfelder, wie diese bei der Behandlung von supradiaphragmatischen malignen Lymphome mittels Cobalt 60 hier üblich sind, wurden studiert. Es wurden Isodosenpläne für Mantelfelder in der Sagittalebene und in verschiedenen Transversalebenen konstruiert. An einem Thoraxphantom wurde das Übereinstimmen der geplanten Dosen und der wirklich gemessenen Dosis mit und ohne dem Gebrauch von Ausgleichsfiltern geprüft.

RÉSUMÉ

L'auteur a analysé la dosimétrie des champs en mantelet pour le traitement des lymphomes malins sus-diaphragmatiques par le cobalt 60. Elle a construit des courbes isodoses pour le champ en mantelet dans un plan sagittal et dans différents plans transversaux. Elle a étudié la concordance entre les doses prévues et les doses mesurées sur un fantôme de thorax avec et sans filtre compensateur du faisceau.

REFERENCES

BRUCE W. R. and JOHNS H. E.: The spectra of X rays scattered in low atomic number materials. Brit. J. Radiol. (1960) Suppl. No. 9.

CLARKSON J. R.: A note on depth doses in fields of irregular shape. Brit. J. Radiol. 14 (1941), 265.

CRAVER L. F.: Some aspects of the treatment of Hodgkin's disease. Cancer 7 (1954), 927.

DAHL O. and VIKTERLÖF K. J.: Attainment and value of precision in deep radiotherapy. Acta radiol. (1960) Suppl. No. 189.

DEPTH DOSE TABLES FOR USE IN RADIOTHERAPY. Brit. J. Radiol. (1961) Suppl. No. 10.

DUTREIX A. et DUTREIX J.: Construction des isodoses pour les surfaces obliques et irrégulières. J. Radiol. Électrol. 43 (1962), 671.

EASSON E. C. and RUSSEL M. H.: The cure of Hodgkin's disease. Brit. med. J. 1963: I, p. 1704.

GUPTA S. K. and CUNNINGHAM J. R.: Measurement of tissue-air ratios and scatter functions for large field sizes for cobalt 60 gamma radiation. Brit. J. Radiol. 39 (1966), 7.

JELLIFFE A. M.: The present place of radiotherapy in the cure of Hodgkin's disease. Clin. Radiol. 16 (1965), 274.

KAPLAN H. S.: The radical radiotherapy of regionally localized Hodgkin's disease. Radiology 78 (1962), 553.

— Role of intensive radiotherapy in the management of Hodgkin's disease. Cancer 19 (1966), 356.

LANDBERG T.: Clinical course of Hodgkin's disease treated with radiotherapy. Acta radiol. Ther. Phys. Biol. 8 (1969), 487.

— und LARSSON L.-E.: Studium des klinischen Verlaufs bei Sternberg'scher Erkrankung. Radiol. Austr. 18 (1968), 197.

MUSSHOFF K. and BOUTIS L.: Therapy results in Hodgkin's disease, Freiburg im Breisgau 1948—1966. Cancer 21 (1968), 1100.

NEWALL J.: The management of Hodgkin's disease. Clin. Radiol. 1 (1965), 40.

PETERS M. V.: Prophylactic treatment of adjacent areas in Hodgkin's disease. Cancer Res. 26 (1966), 1232.

ROSENBERG S. A. and KAPLAN H. S.: Evidence for an orderly progression in the spread of Hodgkin's disease. Cancer Res. 26 (1966), 1225.